The 390 cm feature of polycrystalline Hematite – an optical crystallite size effect

Thomas G. Mayerhöfer, Jürgen Popp

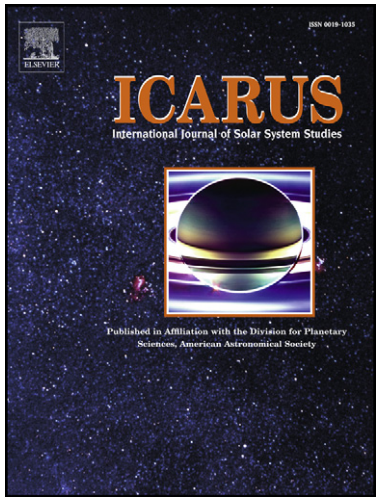

The 390 cm $^{-1}$ feature of polycrystalline Hematite – an optical crystallite size effect

Thomas G. Mayerhöfer, Jürgen Popp

PII: S0019-1035(09)00177-8
DOI: 10.1016/j.icarus.2009.03.039
Reference: YICAR 9007

To appear in: *Icarus*

Received Date: 10 December 2007
Revised Date: 21 January 2009
Accepted Date: 20 March 2009

Please cite this article as: Mayerhöfer, T.G., Popp, J., The 390 cm $^{-1}$ feature of polycrystalline Hematite – an optical crystallite size effect, *Icarus* (2009), doi: 10.1016/j.icarus.2009.03.039

The 390 cm^{-1} feature of polycrystalline Hematite – an optical crystallite size effect

Thomas G. Mayerhöfer[1,2] and Jürgen Popp[1,2]
1: Institut für Physikalische Chemie, Friedrich-Schiller-Universität, Lessingstraße 10, D-07743 Jena, Germany
2: Institut für Physikalische Hochtechnologie e.V., Albert-Einstein-Str. 9, D-07745 Jena, Germany

Crystallite size effect in polycrystalline hematite

PD Dr. Thomas Mayerhöfer (Thomas.Mayerhoefer@ipht-jena.de)
Institut für Photonische Technologien
Albert-Einstein Str. 9
D-07745 Jena
Germany
Phone: +49-3641-206326
Fax: +49-3641-206099

Abstract

The 390 cm^{-1} spectral feature of polycrystalline hematite is shown to be caused by a crystallite size effect which caused by the anisotropic nature of single crystalline hematite. This effect occurs if the probing light is able to resolve the heterogeneous nature of a polycrystalline material and if the corresponding single-crystalline material is optically anisotropic. Therefore it does not depend on whether the material of interest is powder or consolidated. As a consequence, the resulting macroscopic reflectance and transmittance of the polycrystalline material is an average of the microscopic reflectance and transmittance of the individual crystallites. Therefore, randomly oriented polycrystalline materials with large crystallites show characteristic changes in their spectral profile compared to that of polycrystalline materials consisting of crystallites that are small in comparison with the wavelength. The extent of the spectral changes depends on the degree of optical anisotropy of the corresponding single crystalline material. The spectral changes also comprise non-zero cross-polarization terms despite of random orientation. Therefore a characterization of a polycrystalline material with a scalar dielectric function is possible in general only if a polycrystalline material consists of randomly oriented crystallites small compared to the wavelength.

Spectroscopy, Infrared Observations, Mineralogy

1. Introduction

Laboratory characterization of terrestrial analogues of planetary and stellar materials is a fundamental and important step towards the analysis and understanding of remote sensing data recorded by space instrumentation or ground-based observations. The surfaces of solid stellar objects usually consist of polycrystalline materials in a more or less randomly oriented form. E.g. midinfrared spectra of these materials often show features, which may vary depending on the grain and crystallite size [*Aronson and Emslie,* **1973**, *Lane and Christensen,* 1998, Lane *1999*] and may not be present in the principal spectra of the corresponding single crystalline forms (principal spectra are those, which were recorded with the polarization direction of the incident light being parallel to one of the Eigenvectors of the dielectric tensor; for orthorhombic or higher crystal symmetry these coincide with the crystallographic axes). An important and well-known example is polycrystalline hematite and the differences in the infrared spectra of coarse- and fine grained (submicron) form consisting especially of the prominent 390 cm^{-1} feature [*Estep-Barnes* 1977, *Rendon and Serna* 1981, *Christensen et al.* 2000, *Lane et al*. 2002]. To be more precise, the existence of this feature is not linked with the grain, but with the crystallite size in relation to the wavelength of light. It is absent in the spectra of polycrystalline hematite with randomly-oriented crystallites that are small compared to the wavelength and in the principal spectra of the single crystal [*Lane et al.* 2002, *Glotch et al.* 2006]. The absence of the 390 cm^{-1}-band in the principal spectra of the single crystal is an indication for the lack of an excitation of a transverse optical phonon at or around 390 cm^{-1}.

So far, in our view a comprehensive explanation for the existence of this feature is still missing in the literature. It is the aim of this paper to not only provide this explanation but also to point out that the existence of the 390 cm^{-1} band in hematite is based on an optical crystallite size-effect, which concerns all randomly-oriented polycrystalline materials with the exception of the minority the corresponding single crystals of which belong to the cubic crystal system. A comprehensive understanding of this crystallite size-effect has been provided recently [*Mayerhöfer* 2004]. While this understanding allows the modeling of spectra of the polycrystalline species from single crystal data, it also reveals that randomly-oriented (i. e. optically isotropic) polycrystalline materials, which do not exclusively consist of crystallites that are small compared with the wavelength, cannot generally be characterized by a scalar dielectric function (the only exception are polycrystalline materials with

corresponding single crystals with cubic crystal symmetry as mentioned above) [*Mayerhöfer et al.* 2005].

2. Theory

Despite of the fact that randomly oriented polycrystalline materials are always macroscopically optically isotropic, the key for the understanding of their optical properties and their spectral patterns can be found in the optics of anisotropic materials, i.e. the corresponding single crystals. The basic principles, which are also essential to understand the optics of polycrystalline materials with large crystallites, will be introduced shortly in the next paragraph.

2.1 Reflectance and transmittance from a single crystal specimen

The optical properties of a crystal can be specified by its complex dielectric function tensor ε assumed that the crystal is non-magnetic ($\mu = 1$). In the intrinsic coordinate system *x*,*y*,*z* of the crystal (in case of crystals with orthorhombic or higher symmetry, it is convenient to define the intrinsic coordinate system in a way that *x* ∥ *a*, *y* ∥ *b*, *z* ∥ *c*, where *a*,*b*,*c* are the crystallographic axes) its dielectric function tensor is given by

$$\varepsilon = \begin{pmatrix} \varepsilon_a & 0 & 0 \\ 0 & \varepsilon_b & 0 \\ 0 & 0 & \varepsilon_c \end{pmatrix}, \tag{1}$$

where ε_a, ε_b and ε_c are the principal dielectric functions. Relative to a reference frame (e.g. the laboratory coordinates *X*,*Y*,*Z*) the dielectric function tensor is represented in general by

$$\varepsilon(X,Y,Z) = \mathbf{A}(\Omega)\begin{pmatrix} \varepsilon_a & 0 & 0 \\ 0 & \varepsilon_b & 0 \\ 0 & 0 & \varepsilon_c \end{pmatrix}\mathbf{A}(\Omega)^{-1}. \tag{2}$$

Here, **A** is a rotation matrix depending on the orientation Ω, which may be specified e.g. by one of the 24 Euler orientation representations employing the so-called Euler angles φ,θ,ψ [*Mayerhöfer*, 2005].

We assume in the following that an optically flat surface of the crystal is oriented parallel to the *X*-*Y* plane. If the *Y*-*Z*-plane of the laboratory coordinate system is chosen as the plane of incidence, then the angle between the ray direction in the incidence medium and the *Z*-axis is known as the angle of incidence α. Illuminating the crystal's surface, the Z-component of its wavevector $\vec{k}$ inside the material, γ, is linked to the material property $\varepsilon(X,Y,Z)$. One way to describe this linkage is given by eqn. (3),

$$\det\left|\begin{pmatrix} \varepsilon_{XX} - \sin^2\alpha - \gamma^2 & \varepsilon_{XY} & \varepsilon_{XZ} \\ \varepsilon_{YX} & \varepsilon_{YY} - \gamma^2 & \varepsilon_{YZ} + \gamma\sin\alpha \\ \varepsilon_{ZX} & \varepsilon_{ZY} + \gamma\sin\alpha & \varepsilon_{ZZ} - \sin^2\alpha \end{pmatrix}\right| = 0, \tag{3}$$

resulting in a quartic equation in γ with four solutions $\gamma_{\pm 1}$ and $\gamma_{\pm 2}$ (explicit solutions for $\gamma_{\pm 1}$ and $\gamma_{\pm 2}$ can be found in [*Mayerhöfer*, 2004]; they have in general a very extensive and complicated form). Inserting these solutions consecutively into equation (4), and solving simultaneously two of the three resulting equations, solutions of two components of the electric field **E** are obtained in terms of a third, which is arbitrary.

$$\begin{pmatrix} \varepsilon_{XX} - \sin^2\alpha - \gamma^2 & \varepsilon_{XY} & \varepsilon_{XZ} \\ \varepsilon_{YX} & \varepsilon_{YY} - \gamma^2 & \varepsilon_{YZ} + \gamma\sin\alpha \\ \varepsilon_{ZX} & \varepsilon_{ZY} + \gamma\sin\alpha & \varepsilon_{ZZ} - \sin^2\alpha \end{pmatrix} \cdot \begin{pmatrix} E_X \\ E_Y \\ E_Z \end{pmatrix} = 0 \tag{4}$$

In eqn. (4), E_x, E_y and E_z represent the polarization directions inside the crystal.

To calculate the reflectance and transmittance we will use in the following the 4×4 matrix formalism that goes back to Yeh [*Yeh*, 1988].
From the polarization directions a transfer matrix **M** can be computed, which links the amplitudes of the incident, reflected and transmitted waves (for a more detailed representation, the interested reader is referred to [*Mayerhöfer and Popp*, 2006b]):

$$\begin{pmatrix} A_s \\ B_s \\ A_p \\ B_p \end{pmatrix} = \begin{pmatrix} M_{11} & M_{12} & M_{13} & M_{14} \\ M_{21} & M_{22} & M_{23} & M_{24} \\ M_{31} & M_{32} & M_{33} & M_{34} \\ M_{41} & M_{42} & M_{43} & M_{44} \end{pmatrix} \begin{pmatrix} C_s \\ 0 \\ C_p \\ 0 \end{pmatrix} \tag{5}$$

Here A_s and A_p are the field amplitudes of the incident beam with perpendicularly (*s*-) and parallelly (*p*-)polarized radiation, respectively. Analogously, *B* and *C* denote the amplitudes of the reflected and transmitted waves. The reflection and transmission coefficients r_{ss} and t_{ps} can then be calculated, e.g., as follows (here the first subscript indicates the orientation of the polarizer, whereas the second subscript refers to the orientation of the analyzer):

$$\begin{aligned} r_{ss} &= \left(\frac{B_s}{A_s}\right) = \frac{M_{21}M_{33} - M_{23}M_{31}}{M_{11}M_{33} - M_{13}M_{31}} \\ t_{ps} &= \left(\frac{C_s}{A_p}\right) = \frac{-M_{13}}{M_{11}M_{33} - M_{13}M_{31}} \end{aligned} \tag{6}$$

(relations for the three other reflection and transmission coefficient can be found in [*Yeh*, 1988]).
The reflectances R_{ii} ($i = s,p$) is then given by

$$R_{ii} = \left|r_{ii}\right|^2 . \tag{7}$$

If, for example, only a polarizer is employed, the corresponding reflectances R_s and R_p can be calculated according to:

$$\begin{aligned} R_s &= R_{ss} + R_{sp} = \left|r_{ss}\right|^2 + \left|r_{sp}\right|^2 \\ R_p &= R_{pp} + R_{ps} = \left|r_{pp}\right|^2 + \left|r_{ps}\right|^2 \end{aligned} \tag{8}$$

Explicit expressions for the reflectance R_i (and the Transmittance T_i) can be derived in principle, but are usually quite complex. This complexity is increased further if a single crystal cannot be considered as thick as is often the case in non-absorbing spectral regions. On the other hand, the expressions are drastically simplified under special conditions, i.e. for normal incidence ($\alpha = 0$), high symmetry and / or special orientations of the single crystal. If, e.g. a single crystal is of uniaxial symmetry ($\varepsilon_a = \varepsilon_b$), then the orientation of its optical axis, which is coincident with the crystallographic *c*-axis, needs only two angles φ,θ to be specified

as shown in Figure 1. Assuming normal incidence the resulting equations for the reflection coefficients for an optically thick single crystal (semi-infinite medium) are given by,

$$\begin{aligned} r_{XX} &= r_1 \cos^2\varphi + r_2 \sin^2\varphi \\ r_{XY} &= (r_1 - r_2)\cos\varphi\sin\varphi \\ r_{YY} &= r_1 \sin^2\varphi + r_2 \cos^2\varphi \\ r_{YX} &= (r_1 - r_2)\cos\varphi\sin\varphi \quad , \\ r_i &= \frac{n_i - 1}{n_i + 1}, \\ n_1 &= n_{ord} = \sqrt{\varepsilon_a} \\ n_2 &= \sqrt{\frac{\varepsilon_a \varepsilon_c}{\varepsilon_a \sin^2\theta + \varepsilon_c \cos^2\theta}} \end{aligned} \tag{9}$$

and the result for the corresponding one-polarizer experiment is according to eqn. (8):

$$\begin{aligned} R_X &= R_1(n_1)\cos^2\varphi + R_2(n_2)\sin^2\varphi \\ R_i(n_i) &= |r_i(n_i)|^2 = \left(\frac{n_i - 1}{n_i + 1}\right)^2 \end{aligned} \quad , \tag{10}$$

In general, two waves are generated inside the crystals with mutual perpendicular polarization directions and different paths. In case of the reflected waves the paths coincide. However, linear polarized incident light will generally be elliptically polarized after reflection (R_{sp}, $R_{ps} \neq 0$). The cross polarization terms R_{sp} and R_{ps} vanish only under certain special conditions:

1. Optically uniaxial crystals (tetragonal, trigonal, hexagonal): The optical axis must be either confined within the plane of incidence or has to be oriented perpendicular to it.
2. Orthorhombic crystal symmetry: All three dielectric axes must be oriented either parallel or perpendicular to the plane of incidence.
3. Monoclinic symmetry: The monoclinic *b*-axis (the dielectric axis the orientation of which is not dependent on frequency) has to be oriented parallel to the interface and either parallel or perpendicular to the plane of incidence.
4. Triclinic symmetry: There are no orientations, which lead to R_{sp}, $R_{ps} = 0$.

If we now consider polycrystalline materials, two principal cases must be distinguished if the corresponding crystals are of a non-cubic symmetry (in case of cubic crystal symmetry these cases coincide):

1. All crystallites are large compared to the wavelength λ of the incident light
2. All crystallites are small compared to the wavelength λ of the incident light

In accordance with effective medium theories [*Mayerhöfer and Popp*, 2006a; *Bohren and Huffman*, 1983] we classify small crystallites as those being small compared to wavelength or having a crystallite diameter $d < \lambda/10$. This classification is supported by experimental results [*Mayerhöfer*, 2004]. As a consequence, at 10 microns (infrared range) crystallites with a diameter smaller than 1 micron are denoted as small, whereas at 400 nm (blue light), the critical crystallite diameter would be 40 nm (note that there is naturally a difference between "grain size" and "crystallite size", since a grain can consist of more than one crystallite!). In order to get to the essence of the optical crystallite size effect, we make some assumptions, some of which were also implicitly contained in the above treatment of the transmission and reflection of single crystals.

In the following, we focus on semiinfinite dense media consisting of randomly oriented and linearly birefringent (and, consequently, dichroic) ordered regions (crystallites). This means

that we are essentially interested in spectral regions, where the media are absorptive, so that light does not penetrate and leave the samples at the backside (also: no multiple reflections). Besides, their density should be close to the density of the corresponding single crystals (no hollow spaces inside the samples). In addition, we employ vacuum as the incidence medium (index of refraction of the incidence medium $n_{inc} = 1$) and suppose the interface between incidence medium and sample to be smooth (no surface roughness, no holes).

2.2 Reflectance and transmittance from a randomly oriented polycrystalline material with optically small crystallites

In the small crystallite case, the general assumption of the textbooks of Optics, which is that the dielectric tensor of the crystallites is averaged to a scalar and the material is isotropic, is correct: When inspected through a microscope, the heterogeneous nature of the sample is not revealed, since the material is characterized everywhere by the same dielectric function. This also means that if viewed with a polarizing microscope with polarizer and analyzer crossed, no intensity can be detected. The question at hand however is, how is the dielectric tensor of the individual crystallites reduced to a scalar? In other words, if the dielectric tensor of the single crystal is known, how can the scalar dielectric function ε_{av} of the polycrystalline material be computed? A simple approach would be to calculate the arithmetic mean of either the principal dielectric functions ε_a, ε_b and ε_c or the principal indices of refraction n_a, n_b and n_c (with $n_i^2 = \varepsilon_i$) according to

$$\langle \varepsilon \rangle = \frac{1}{3}\varepsilon_a + \frac{1}{3}\varepsilon_b + \frac{1}{3}\varepsilon_c \tag{11}$$

and

$$\langle n \rangle = \frac{1}{3}n_a + \frac{1}{3}n_b + \frac{1}{3}n_c \tag{12}$$

with $\varepsilon_{av} = \langle n \rangle^2$. Obviously eqs. (11) and (12) are contradictory to each other as $\langle \varepsilon \rangle \neq \varepsilon_{av}$ [*Mayerhöfer and Popp*, 2006a]. Since especially simulations based on eqn. (11) only very poorly resemble experimental spectra (the larger the differences between ε_a, ε_b and ε_c, the poorer is the resemblance [*Mayerhöfer*, 2002]), it is evident that more sophisticated approaches have to be employed. Such an approach is the effective medium approximation (EMA), which was recently extended to be able to handle crystallites of monoclinic and triclinic symmetry [*Mayerhöfer and Popp*, 2007].

EMA is an extension of eqn. (10) in a way that it assumes a polydomain medium to consist of three individual materials, the mutual interaction being dictated by electrostatics and the dielectric functions of which are the three principal dielectric functions of the corresponding single crystal [*Mayerhöfer*, 2002]. Its results are in accordance with those of scattering theories for domains small compared with the wavelength [*Bohren and Huffman*, 1983]. Originally EMA was applied to calculate effective optical constants of heterogenic materials consisting of two or more different phases (without distinction between inclusion and matrix).

Presuming that the domains are of spherical shape an averaged dielectric function $\langle\varepsilon\rangle$ can be obtained from the following relation,

$$\begin{aligned}
&\tfrac{1}{3}\frac{\varepsilon_a-\langle\varepsilon\rangle}{\varepsilon_a+2\langle\varepsilon\rangle}+\tfrac{1}{3}\frac{\varepsilon_b-\langle\varepsilon\rangle}{\varepsilon_b+2\langle\varepsilon\rangle}+\tfrac{1}{3}\frac{\varepsilon_c-\langle\varepsilon\rangle}{\varepsilon_c+2\langle\varepsilon\rangle}=0\\
&\rightarrow\langle\varepsilon\rangle^3-\frac{1}{4}\left(\varepsilon_a\varepsilon_b+\varepsilon_b\varepsilon_c+\varepsilon_c\varepsilon_a\right)\langle\varepsilon\rangle+\frac{1}{4}\varepsilon_a\varepsilon_b\varepsilon_c=0\\
&\rightarrow\langle\varepsilon\rangle^3-\frac{1}{4}K_1\langle\varepsilon\rangle+\frac{1}{4}K_2=0 \qquad ,\\
&K_1=\varepsilon_a\varepsilon_b+\varepsilon_b\varepsilon_c+\varepsilon_c\varepsilon_a\\
&K_2=\varepsilon_a\varepsilon_b\varepsilon_c
\end{aligned} \tag{13}$$

with in general three solutions:

$$\begin{aligned}
\langle\varepsilon\rangle_1&=-\frac{3^{\frac{1}{3}}K_1+K_3^{\frac{2}{3}}}{2\times3^{\frac{2}{3}}K_3^{\frac{1}{3}}}\\
\langle\varepsilon\rangle_2&=-\frac{2(-3)^{\frac{1}{3}}K_1+\left(1-i\sqrt{3}\right)K_3^{\frac{2}{3}}}{4\times3^{\frac{2}{3}}K_3^{\frac{1}{3}}}\\
\langle\varepsilon\rangle_3&=-\frac{3^{\frac{1}{3}}\left(1-i\sqrt{3}\right)K_1+\left(1+i\sqrt{3}\right)K_3^{\frac{2}{3}}}{4\times3^{\frac{2}{3}}K_3^{\frac{1}{3}}}.
\end{aligned} \tag{14}$$

$$K_3=-9K_2+\sqrt{3}\sqrt{27K_2^{\,2}-K_1^{\,3}}$$

Starting from principal dielectric functions of the form $\varepsilon_j=\varepsilon_{j,1}+i\varepsilon_{j,2}$, where the $\varepsilon_{j,1}$ are the real parts and $\varepsilon_{j,2}$ are the imaginary parts, for any wavenumber only one of the solutions $\langle\varepsilon\rangle_1$ to $\langle\varepsilon\rangle_3$ has a positive imaginary part and is therefore the solution, which must be chosen.
For optically uniaxial materials ($\varepsilon_a=\varepsilon_b$) eqn. (14) simplifies to

$$\langle\varepsilon\rangle=1/4\left(\varepsilon_a+\sqrt{\varepsilon_a}\sqrt{\varepsilon_a+8\varepsilon_c}\right). \tag{15}$$

An alternative theory with a completely different theoretical foundation, leading however to similar results [*Mayerhöfer and Popp* 2006a], is the so-called average refractive index theory (ARIT). According to ARIT the index of refraction $\langle n\rangle$ of a polycrystalline material is an orientational average of the two indices of refraction $n_1(\Omega)$ and $n_2(\Omega)$ of the crystallites and given by [*Mayerhöfer* 2004]:

$$\langle n\rangle=N^{(3)}\int_{\Omega^{(3)}}\left(\frac{n_1(\Omega)}{2}+\frac{n_2(\Omega)}{2}\right)d\Omega \tag{16}$$

$N^{(3)}$ represents a normalization factor given by $N^{(3)}=(\int_{\Omega^{(3)}}d\Omega)^{-1}$ and Ω represents the orientation, which can be expressed e.g. with one of the Symmetric Euler Orientation

Representations [*Mayerhöfer* 2005]. The indices of refraction $n_1(\Omega)$ and $n_2(\Omega)$ can be calculated by eqn. (3) setting $\alpha = 0$, since then the Z-components of $\vec{k}$ equal the indices of refraction.
In case of optical uniaxial crystallites, one index of refraction is independent of orientation and the second depends on the angles φ and θ. Therefore $\langle n \rangle$ is given by:

$$\begin{aligned} \langle n \rangle == & \frac{1}{2}\left(n_1 + \frac{1}{2\pi^2} \int_0^{\pi/2} \int_0^{\pi/2} n_2 \; d\varphi d\theta \right) \\ n_1 = & \sqrt{\varepsilon_a} \\ n_2 = & \sqrt{\frac{\varepsilon_a \varepsilon_c}{\varepsilon_a \left(\cos^2\theta + \cos^2\varphi \sin^2\theta \right) + \varepsilon_c \sin^2\varphi \sin^2\theta}} \end{aligned} \tag{17}$$

Transmittance, reflectance and emittance can then be calculated using the well-known Fresnel equations.

2.3 Reflectance and transmittance from a randomly oriented polycrystalline material with optically large crystallites

In the large crystallite case, a randomly oriented material is still optically isotropic. However, inspecting the sample with a microscope with wavelengths small compared to the crystallite size reveals that the material is heterogeneous, as the micro-spectra depend in this case on the position of the light beam on the surface (since only one or a few crystallites with varying orientations are within the spot of the light beam) and on the magnification (the larger the spot, the more crystallites are covered and the spectrum increasingly resembles that gained from a large area), which means that the material is no longer microscopically, but still macroscopically isotropic. Accordingly, the reflectance of the polycrystalline material $\langle R \rangle$ is now the orientational average of the individual reflectances $R(\Omega)$ of the crystallites [*Mayerhöfer* 2004]:

$$\langle R \rangle = N^{(3)} \int_{\Omega^{(3)}} R(\Omega) \, d\Omega = N^{(3)} \int_{\Omega^{(3)}} \left(\frac{R_s(\Omega)}{2} + \frac{R_p(\Omega)}{2} \right) d\Omega \tag{18}$$

Here, $R_s(\Omega)$ and $R_p(\Omega)$ represent the reflectances with perpendicularly (s-)polarized and parallel (p-)polarized *incident* light. Since the individual crystallites are assumed to be anisotropic, as they are for hematite, $R(\Omega)$ has to be calculated e.g. by applying a 4×4 matrix formalism (eqs. (3)-(8)). As a result of the averaging, the directional dependency of the optical properties vanishes. However, $R_s(\Omega)$ is the sum of two reflectance terms $R_{ss}(\Omega)$ and $R_{sp}(\Omega)$ (the second subscript reflects the orientation of the polarization of the reflected light), i.e. $R_s(\Omega) = R_{ss}(\Omega) + R_{sp}(\Omega)$. From this result it can be seen that the cross-polarization terms $\langle R_{sp} \rangle$ and $\langle R_{ps} \rangle$ cannot be equal to zero, since $R_{sp}(\Omega)$ and $R_{ps}(\Omega)$ are zero only for so-called principal orientations of the crystallites as already discussed in section 2.1 (viewed under a microscope with crossed polarizers only those crystallites would not be visible, which possess principal orientations). Therefore, the optical properties of polycrystalline materials with large crystallites in general cannot be characterized by a scalar dielectric function, even

if the crystallites are randomly oriented (the only exception are polycrystalline materials the corresponding single crystals of which are of cubic symmetry with $\varepsilon_a = \varepsilon_b = \varepsilon_c$).
For uniaxial symmetry and normal incidence eqn. (18) transforms by use of eqs. (9) and (10) into:

$$\begin{aligned}\left\langle R(\alpha=0)\right\rangle_{uniaxial} &= \frac{4}{\pi^2}\int_{\theta=0}^{\pi/2}\int_{\varphi=0}^{\pi/2}\left[R_1(n_1)\cos^2\varphi + R_2(n_2)\sin^2\varphi\right]d\varphi\, d\theta = \\ &= \frac{1}{\pi}\int_{\theta=0}^{\pi/2}\left[R_1(n_1)+R_2(n_2)\right]\,d\theta = \\ &= \frac{1}{2}R_1(n_1)+\frac{1}{\pi}\int_{\theta=0}^{\pi/2}\left[R_2(n_2)\right]\,d\theta\end{aligned} \quad . \tag{19}$$

3. Results and Discussion

Especially for the understanding and interpretation of spectra recorded from polycrystalline materials with large crystallites, it is important to discuss first the changes that spectra of the single crystal undergo when the orientation of a single crystal changes, e.g. when the angles φ and θ are varied for optically uniaxial crystals. The so-called principal spectra can be obtained when a *c*-axis cut of the crystal is employed (in a *c*-axis cut, the crystallographic *c*-axis of the crystal is oriented parallel to the surface). Referring to Fig. 1, this means that the *c*-axis is oriented parallel to the interface and that the angle θ takes on the value 90°. Assuming normal emittance (this means that the emitted light beam travels along the (negative) *Z*-axis) and employing an analyzer oriented parallel to *X*, one principal spectra is obtained if the *c*-cut of the crystal is oriented according to φ = 0 (*c*-axis of the crystal parallel to the *Y*-axis of the reference frame). In this configuration, $R_X = R_1(n_1)$ based on eqs. (9) and (10), therefore the emittance $\in_X = 1 - R_X$ is only influenced by the principal dielectric function ε_a. The resulting spectrum is usually denoted either as the **E** ∥ *a*- or **E** ⊥ *c*-spectrum. The minima in this spectrum are caused by vibrations that have their transition moment in the *a*-*a* plane and are of E_u symmetry. The second principal spectrum is generated when the *c*-cut is rotated around *Z* by 90° (φ = 90°). Now $R_X = R_2(n_2)$ and $n_2 = \sqrt{\varepsilon_c}$, which means that $\in_X$ is now solely depending on ε_c. This spectrum is generally called the **E** ∥ *c*-spectrum. This spectrum's minima result from vibrations that have their transition moment parallel to the *c*-axis of the crystal and are of A_u symmetry. The principal spectra are depicted in Fig. 2 (the spectra have been calculated from the oscillator data provided by Onari et al. [*Onari et al.* 1977]). None of the spectra shows a band around 390 cm^{-1}, which essentially means in case of a structural interpretation on the unit-cell level that there is neither an oscillator with A_u- nor an oscillator with E_u-symmetry present having an oscillator position around 390 cm^{-1}. Besides, we notice that there is a region of strong optical anisotropy between about 300 and 550 cm^{-1}. In this range there are a number of points where the emittances of both principal spectra are equal. These are so-called isosbestic points [*Ivanovski et al.*, 2008], since all spectra generated by a variation of φ share these points (Fig. 3). The occurrence of isobestic points are a consequence of the form of eqn. (19), which results from eqn. (9) by setting θ = 90°:

$$\begin{aligned}R_X &= R_a(n_a)\cos^2\varphi + R_c(n_c)\sin^2\varphi \\ R_i(n_i) &= \left|r_i(n_i)\right|^2 = \left(\frac{n_i-1}{n_i+1}\right)^2;\quad n_i = \sqrt{\varepsilon_i} \qquad i = a,c\end{aligned} \quad . \tag{20}$$

From the linear combination of the principal spectra $\in_a (=1-R_a)$ and $\in_c (=1-R_c)$ it follows that a variation of φ usually only changes the intensity but not the position of emittance minima. An exception is obviously the region between the isosbestic points at 336 cm^{-1} and at 407 cm^{-1}. In this region an only weekly pronounced minimum develops at about 388 cm^{-1} from shoulders of the adjacent bands for φ = 45°, which vanish at φ = 0 and 90°. This minimum alone cannot be responsible for the 390 cm^{-1} feature in the spectra of large-grained polycrystalline Hematite, otherwise all crystallites would have to possess orientations close to φ = 45°,θ = 90°.

To obtain the full picture, obviously also changes of the spectra of the single crystal with varied θ must be taken into account. These changes are also depicted in Fig. 3. Since θ represents the angle between the crystal's *c*-axis and its projection onto the surface, it would be necessary to prepare one crystal cut for each variation in θ. These cuts would have to be oriented in a way that the projection of the *c*-axis onto the surface of the crystal is oriented parallel to the *X*-axis of the reference frame (cf. Fig. 1) and to the orientation of the polarizer. The spectral variations in dependence of θ are then described by

$$\begin{aligned} R_X &= R_2\left(n_2\right) = \left|r_2\left(n_2\right)\right|^2 = \left(\frac{n_2-1}{n_2+1}\right)^2 \\ n_2 &= \sqrt{\frac{\varepsilon_a \varepsilon_c}{\varepsilon_a \sin^2\theta + \varepsilon_c \cos^2\theta}} \\ \in_X &= 1-R_X \end{aligned} \qquad (21)$$

A key to the understanding of the different spectral variations resulting from changes in θ compared to those initiated by changes in φ, is the fact that as long as θ = 0 or θ = 90° the polarization inside the crystal has no component in the *Z*-direction (E_Z = 0 and **E** and $\vec{k}$ are mutually orthogonal). This is no longer the case for θ ≠ 0, and the waves inside the crystal take on a mixed transversal-longitudinal character and band minimima (band maxima in the reflectance spectra) begin to shift from their tranversal-optical (TO) position towards their longitudinal-optical (LO) position [Loudon, 1964]. This effect is clearly visible in the lower part of Fig. 3 between 300 and 550 cm^{-1}: At θ = 15° a minimum develops at 408 cm^{-1}, which is shifted towards lower wavenumbers with increasing θ. This mimimum belongs to the A_u-vibration with a TO-position of 299 cm^{-1} and an LO-position of 414 cm^{-1} [*Onari et al.*, 1977]. At the same time the minimum at 463 cm^{-1} is gradually shifted towards higher wavenumbers and eventually vanishes at θ = 90°. This minimum belongs to the E_u-vibration with a TO-position of 437 cm^{-1} and a corresponding LO-position at 494 cm^{-1} [*Onari et al.*, 1977].

According to eqs. (18) and (19) the average of all spectra presented in Fig. 3 and, additionally, all spectra for all intermediate orientations contribute to the spectrum of a polycrystalline sample with large crystallites. This can easily be understood by employing again a thought experiment utilizing a microscope: First the magnification may be assumed to be so large that only one crystallite is imaged. Its spectrum resembles that of a single crystal with the same orientation. As the magnification is gradually decreased additional crystallites contribute to the spectrum. Finally the number of crystallites is so large that it resembles that recorded by a usual spectrometer. Depending on the optical anisotropy, the number of crystallites can be as low as 10, which means that an average of 10 different single crystal spectra can already resemble that of a polycrystalline sample in a satisfying manner. Usually at least 500 to 1000 different orientations and corresponding spectra have to be averaged. The artificial spectrum generated from eqn. (19) and shown in the lower part of Fig. 4 was calculated for only 91 different orientations, since for optically uniaxial crystals and normal incidence / emittance the first integral with regard to the angle φ can be solved analytically. Comparing the artificial

spectrum with an experimental spectrum (Fig. 4) it can be noticed that in the range up to 500 cm^{-1} the resemblance is comparably good. The shape of the band around 550 cm^{-1} is less well reproduced. In this region the influence of the surface roughness and the occurrence of holes on the surface and in the volume of real samples lead to deviations between artificial and experimental spectrum due to scattering effects, which are not accounted for in the calculations. These deviations are even more pronounced in case of the experimental sample with small crystallites. These effects are not introduced by the optical anisotropy of Hematite, since in the spectral regions around 550 and 300 cm^{-1} the difference between the principal dielectric functions is comparably small. This is reflected by the small differences between the artificial spectra for small and large crystallites in these regions, whereas in the strongly anisotropic region between 370 cm^{-1} and 500 cm^{-1} strong differences can be noted. These consist in the non-appearance of a minimum in the range around 400 cm^{-1} and in a red-shift of the minimum of the band at about 450 cm^{-1} in the artificial spectrum for a sample consisting of small crystallites based on ARIT (eqn. (19)). Such red-shifts are typical for polycrystalline samples consisting of small crystallites [*Mayerhöfer*, 2004]. They result since the bands for small crystallites samples usually consist of a minimum around the TO-position of the oscillator accompanied by an asymmetric broadening at the high-wavenumber side due to a mixed TO-LO mode character. In contrast, samples with large crystallites generally show bands the maximum of which are shifted towards their LO-positions (except in ranges, where the differences between the principal dielectric functions are small). This blue-shift can also be seen when the experimental spectra in Fig. 4 are compared.

In the region around 400 cm^{-1} the resemblance between experiment and simulation is less favorable for the sample consisting of small crystallites. This result can be explained in principle by three different explanations or combinations thereof.

1. The optical constants of single crystals are generally inadequate for sub-micron crystallites.
2. The employed theory (ARIT) is inadequate to describe the changes due to the crystallite size effect.
3. The missing resemblance is caused by surface roughness, multiple scattering due to the low density of the sample etc.

The first argument was employed in [*Marra et al.*, 2005]. It is contradictory to the observations of Bohren and Huffman [*Bohren and Huffman*, 1983] and also with findings of one of the authors [*Mayerhöfer*, 2004]. In the latter reference the optical properties of polycrystalline samples with exclusively small crystallites were investigated. These were prepared by glass-crystallization resulting in perfectly dense samples with crystallite sizes around 300 nm. It was shown that a small increase of the damping constants by a factor as small as 1.3 is sufficient to characterize the spectral differences between the crystallites and the single crystal. Due to the high quality of the samples spectral effects due to surface roughness, holes and multiple scattering within the sample were completely absent and did not need to be considered. The influence of these effects can be studied in regions where the differences between the principal dielectric functions are small. In these regions the results of the different theories for the generation of an averaged dielectric function should converge. This convergence can indeed be observed below 280 cm^{-1} and above 500 cm^{-1} in the lower part of Fig. 5, which presents a comparison of EMA, ARIT and the simple arithmetic mean of the principal dielectric functions according to eqn. (11). The differences between experimental and modeled spectra in these ranges are therefore due to a missing treatment of multiple scattering effects etc. (the alteration of the band-shape around 600 cm^{-1} is e.g. well-known from polycrystalline samples with rough surfaces [e.g. *Berreman*, 1970; *Pecharromán and Iglesias*, 1994, *Aronson and Emslie*, 1973]), which, of course, will also play an important role in the range between 280 cm^{-1} and above 500 cm^{-1}. In this range, however, effects from surface roughness and multiple scattering are superimposed on the effects resulting from the

optical anisotropy of the crystallites. From the comparison of the spectra generated by the different theories to average the principal dielectric functions with the experimental spectrum, it is therefore in case of ARIT and EMA hardly possible to decide, which theory is superior. The simple arithmetic mean according to eqn. (11), however, is generally inappropriate, since it generates e.g. two peaks around 300 cm^{-1}, while in experimental spectra only one is present (cf. also [*Marra et al.*, 2005]). Besides, the arithmetic mean leads to exaggerated band intensities and to minima that are located between the TO- and LO-frequencies instead of showing a maximum at the TO-frequency. Generally, the arithmetic mean approach is therefore inappropriate except for vanishing differences between the principal dielectric functions [*Mayerhöfer*, 2002].

4. Conclusion

The aim of this paper was to show that for the understanding of the optics of polycrystalline materials, even if they are randomly oriented, an intimate knowledge of the optics of anisotropic materials is generally necessary. Randomly oriented polycrystalline materials that possess exclusively crystallites, which are much smaller than the wavelength of a probing light appear homogenous to it and can therefore be characterized by an averaged dielectric function. This averaged dielectric function can be generated e.g. by ARIT or EMA. Simpler models like the arithmetic mean of the principal dielectric functions can be employed only for vanishing anisotropy.

REFERENCES

Aronson J. R. and Emslie A. G., 1973. Spectral Reflectance and Emittance of Particulate Materials, 2: Application and Results, Appl. Optics 11, 2573 – 2584.

Aronson J. R. and Emslie A. G., 1980. Effective optical constants of anisotropic materials, Appl. Optics 19, 4128 – 4129.

Berreman D. W. 1970. Resonant Reflectance Anomalies: Effect of Shapes of Surface Irregularities, Phys. Rev. B 1, 381 – 389.

Bohren C. F. and Huffman D. R., *Absorption and Scattering of Light by small Particles* (Wiley, New York, 1983).

Christensen P. R., Bandfield J. L., Clark R. N., Edgett K. S., Hamilton V. E., Hoefen T., Kieffer H. H., Kuzmin R. O., Lane M. D., Malin M. C., Morris R. V., Pearl J. C., Pearson R., Roush T. L., Ruff S. W., Smith M. D. 2000. Detection of crystalline hematite mineralization on Mars by the Thermal Emission Spectrometer: Evidence for near-surface water, J. Geophys. Res., 105, 9623 – 9642.

Estep-Barnes, P.A., 1977. Infrared spectroscopy. In: Zussman, J. (Ed.), Physical Methods in Determinative Mineralogy. Academic Press, London, pp. 529–604.

Glotch T. D., Christensen P. R., Sharp T. G., 2006. Fresnel modeling of hematite crystal surfaces and application to martian hematite spherules. Icarus, 181, 408 – 418.

Ivanovski V., Mayerhofer T.G., Popp J., 2008. Isosbestic-like point in the polarized reflectance spectra of monoclinic crystals - A quantitative approach. Spectrochimica Acta A 68, 632 – 638.

Lane M. D., Christensen P. R., 1998. Thermal infrared emission spectroscopy of salt minerals predicted for Mars, Icarus, 135, 528 – 536.

Lane, M.D., 1999. Midinfrared optical constants of calcite and their relationship to particle size effects in thermal emission spectra of granular calcite, J. Geophys. Res., 104, 14099-14108

Lane M. D., Morris R. V., Mertzman S. A., Christensen P. R., 2002. Evidence for platy hematite grains in Sinus Meridiani, Mars. J. Geophys. Res., 107, 5126 – 5140.

Loudon R., 1964. Raman effect in crystals. Adv. Phys. 13, 423 – 482.

Mayerhöfer T. G., 2002. New Method of Modelling IR Spectra of Non-cubic Single-Phase Polycrystalline Materials with Random Orientation. Appl. Spectrosc. 56, 1194-1205.

Mayerhöfer T. G., 2004. Modelling IR-spectra of single-phase polycrystalline materials with random orientation –A unified Approach. Vib. Spectrosc., 35, 67-76.

Mayerhöfer T. G., 2005. Symmetric Euler Orientation Representations for Orientational Averaging. Spectrochimica Acta A 61, 2611-2621.

Mayerhöfer T. G., Shen Z., Keding R., Musfeldt J. L., 2005. Optical isotropy in polycrystalline $Ba_2TiSi_2O_8$: Testing the limits of a well-established concept. Phys. Rev. B, 71, 184116.

Mayerhöfer T. G. and Popp J., 2006a. Effective optical constants: A fundamental discrepancy. Vib. Spectrosc. 42, 118-123.

Mayerhöfer T. G., Popp J., 2006b. Modelling IR-spectra of polycrystalline materials in the large crystallites limit – Quantitative determination of orientation. J. Opt. A: Pure Appl. Opt., 8, 657-671.

Mayerhöfer T. G., Popp J., 2007. Employing spectra of polycrystalline materials for the verification of optical constants obtained from corresponding low symmetry single crystals. Appl. Opt., 46, 327-334.

Onari S., Arai T., Kudo K., 1977. Infrared lattice vibrations and dielectric dispersion in α-Fe_2O_3. Phys. Rev. B, 16, 1717 – 1721.

Pecharromán C. and Iglesias J. E., 1994. A method for the determination of infrared optical constants from reflectance measurements on powdered samples, J. Phys.: Condens. Matt. 6 7125-7141.

Rendon J. L., Serna C. J., 1981. IR-spectra of powder hematite – effects of particle-size and shape, Clay Minerals 16, 375 – 381.

Yeh P., *Optical waves in layered media* (Wiley, New York, 1988)

FIGURE CAPTIONS (color)

FIG. 1. Representation of the orientation of the optical axis by the angles φ and θ.

FIG. 2. Hematite single crystal spectra based on single crystal data provided by Onari et al. [*Onari et al.*, 1977].

FIG. 3. Influence of the orientation on the polarized single crystal spectra (angle of emittance: 0°, upper part: θ = 90°, φ is varied; lower part: φ = 90°, θ is varied).

FIG. 4. Comparison between a) experimental and b) simulated spectra of polycrystalline hematite consisting of optically small (crystallites size $d < \lambda/10$, spectra of sample "Sub-micron (packed)" in Fig. 7 from [*Christensen et al.*, 2000]) or large ($d > \lambda/10$, spectra of sample "HMIR2" in Fig. 7 from [*Lane et al.*, 2002]) crystallites. The experimental spectrum for optically small crystallites has been scaled appropriately (red scale on the right side).

FIG. 5. Comparison of an experimental spectrum of polycrystalline hematite (spectra of sample "Sub-micron (packed)" in Fig. 7 from [*Christensen et al.*, 2000]), with modeled spectra based on ARIT, EMA and eqn. (11).

FIGURE CAPTIONS (bw)

FIG. 1. Representation of the orientation of the optical axis by the angles φ and θ.

FIG. 2. Hematite single crystal spectra based on single crystal data provided by Onari et al. [*Onari et al.*, 1977].

FIG. 3. Influence of the orientation on the polarized single crystal spectra (angle of emittance: 0°, upper part: θ = 90°, φ is varied; lower part: φ = 90°, θ is varied).

FIG. 4. Comparison between a) experimental and b) simulated spectra of polycrystalline hematite consisting of optically small (crystallites size $d < \lambda/10$, spectra of sample "Sub-micron (packed)" in Fig. 7 from [*Christensen et al.*, 2000]) or large ($d > \lambda/10$, spectra of sample "HMIR2" in Fig. 7 from [*Lane et al.*, 2002]) crystallites. The experimental spectrum for optically small crystallites has been scaled appropriately (grey scale on the right side).

FIG. 5. Comparison of an experimental spectrum of polycrystalline hematite (spectra of sample "Sub-micron (packed)" in Fig. 7 from [*Christensen et al.*, 2000]), with modeled spectra based on ARIT, EMA and eqn. (11).

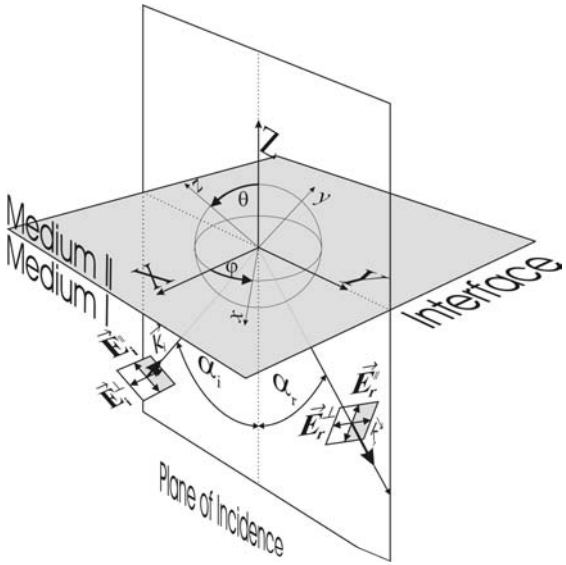

Fig. 1, Mayerhöfer et al.

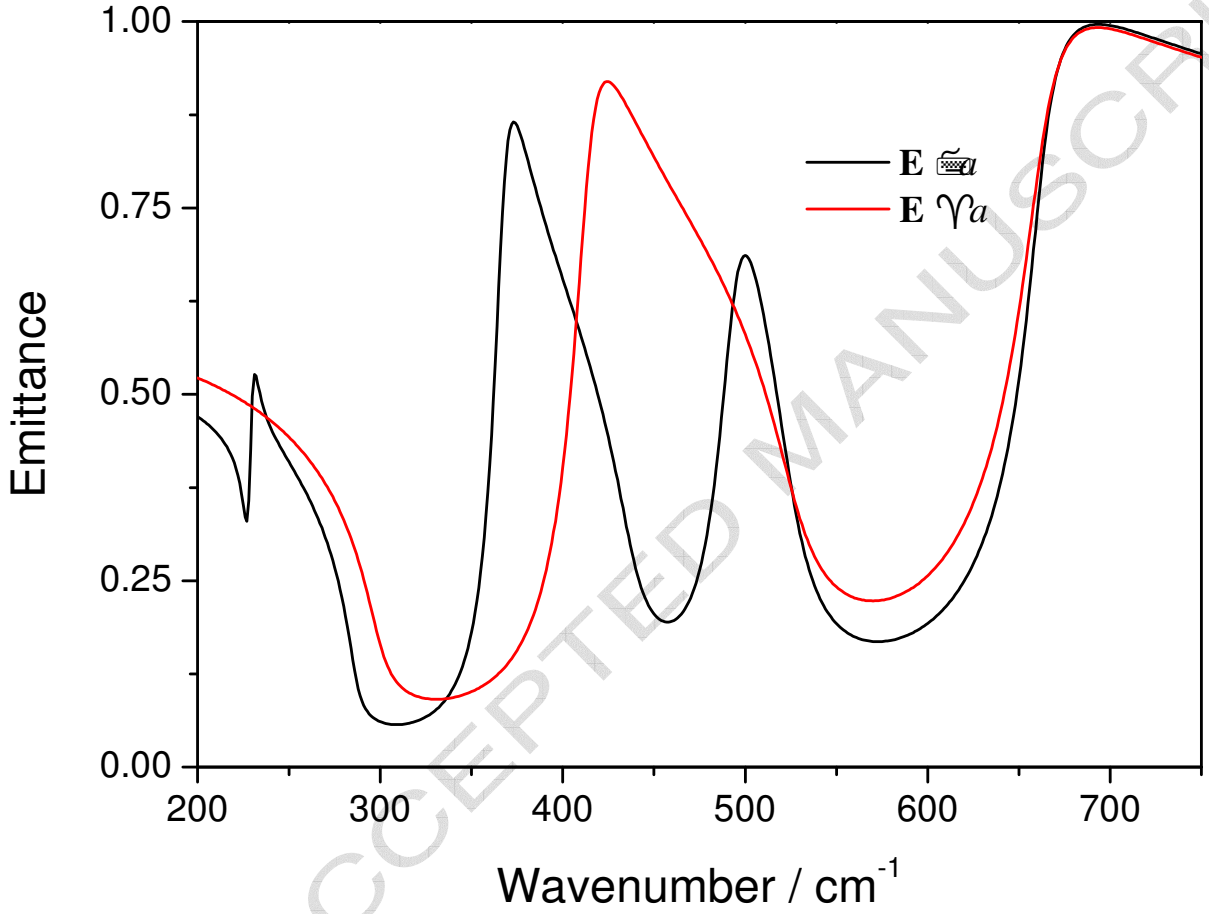

Fig. 2, Mayerhöfer et al.

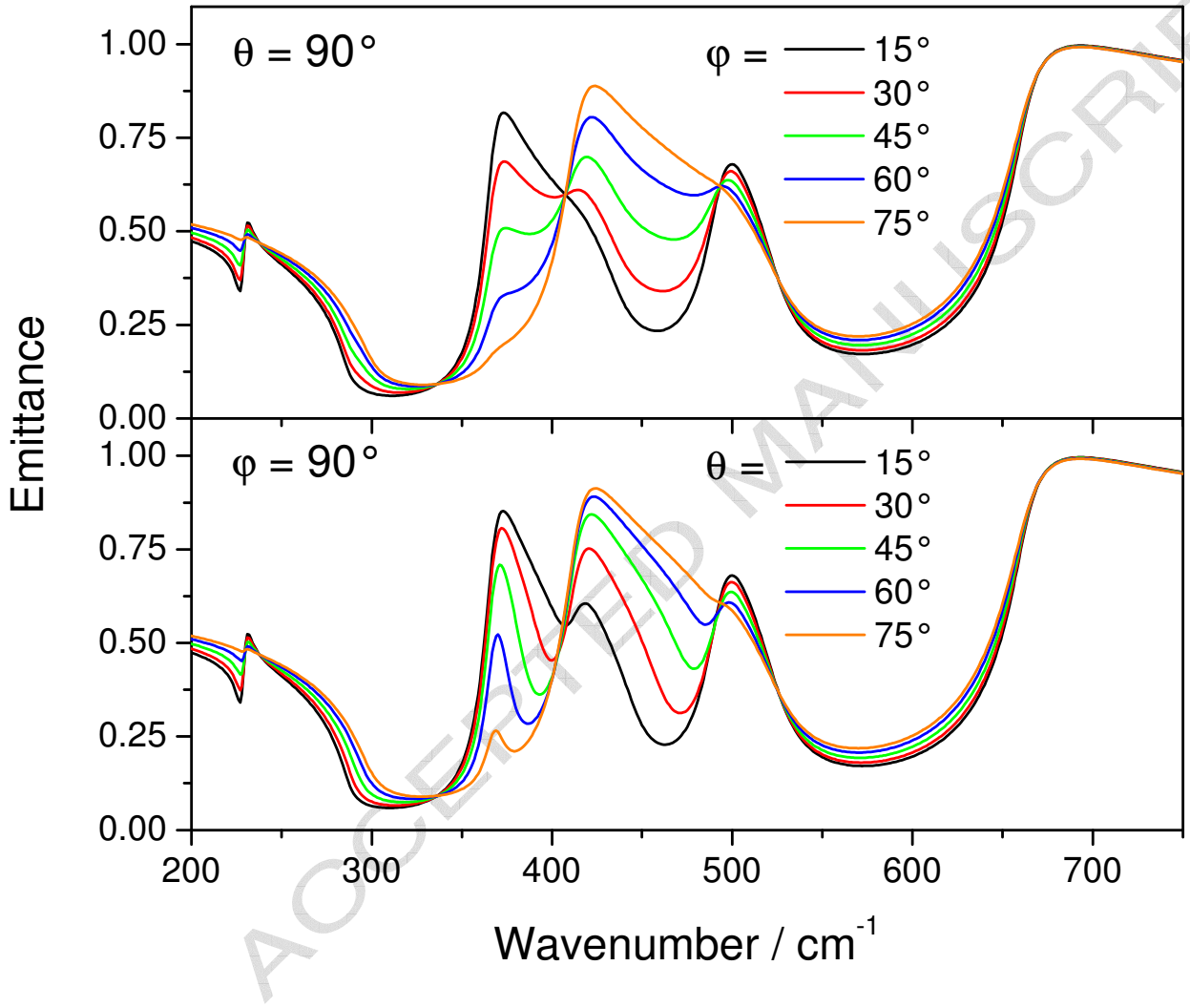

Fig. 3, Mayerhöfer et al.

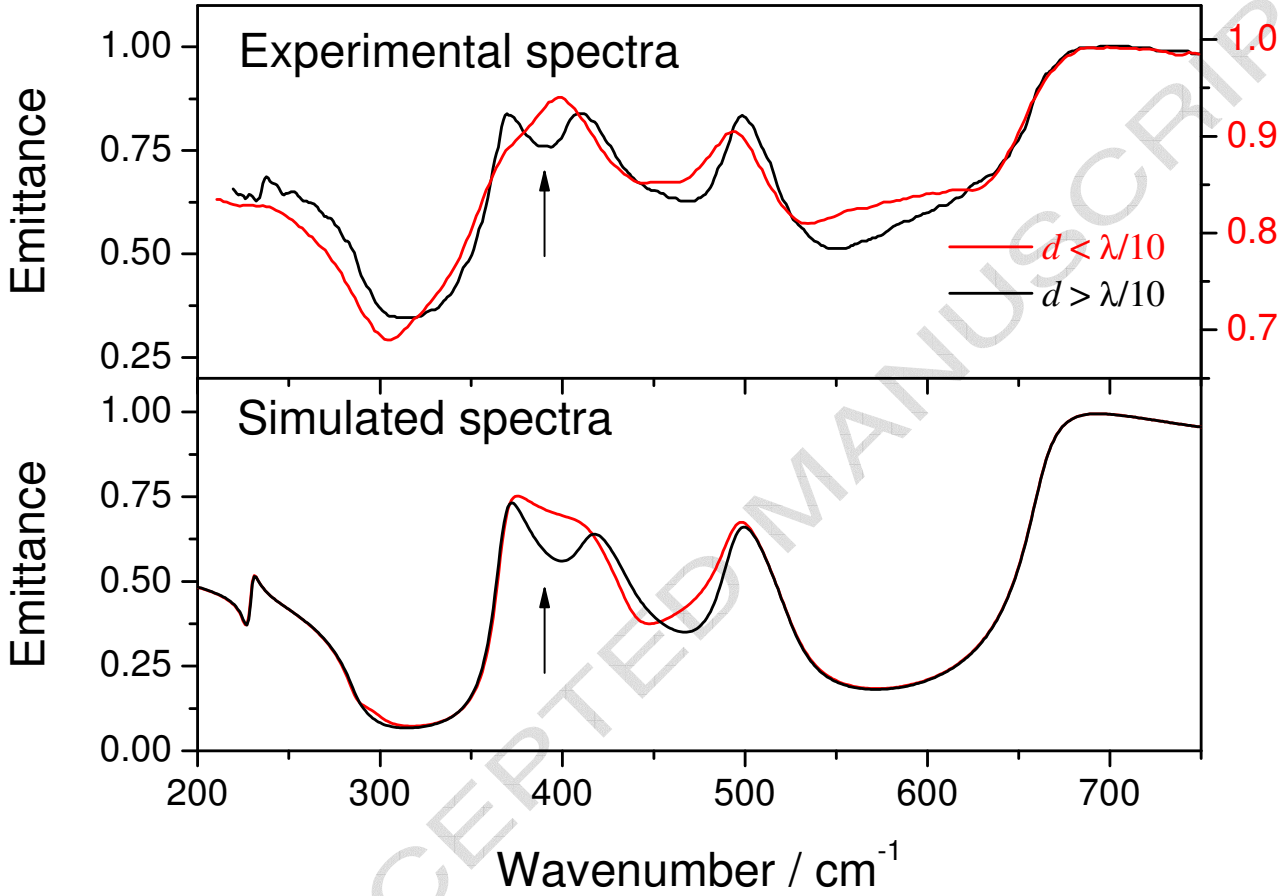

Fig. 4, Mayerhöfer et al.

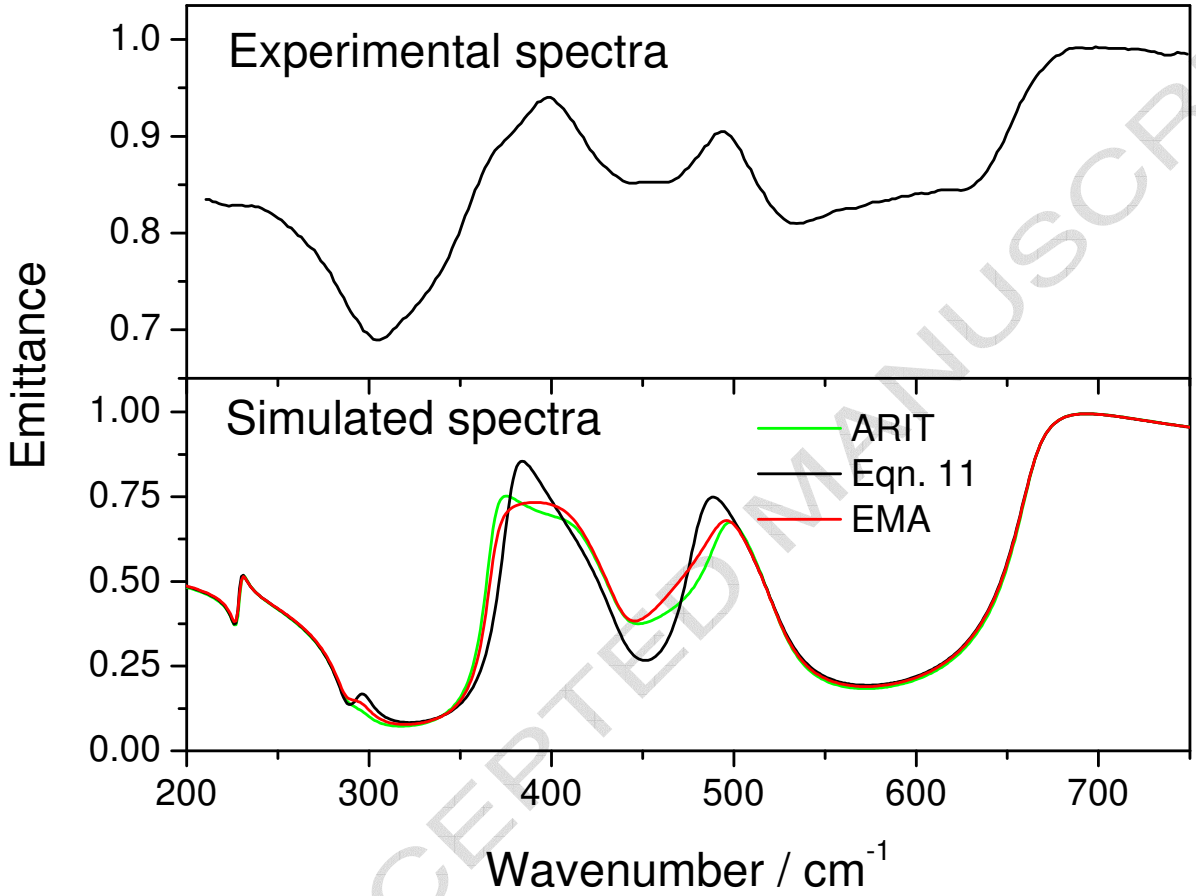

Fig. 5, Mayerhöfer et al.